August 27-31, 2023
FLORENCE - ITALY
ICWE 16
16th International Conference on Wind Engineering

Tornado-like loading on a low-rise building model by a single-celled vortex and a two-celled vortex

Qiang Chen [1], Delong Zuo [2], Zhuo Tang [3], Darryl James [4]

[1~4]*Texas Tech University, Lubbock, TX, USA,* [1]*qiang.chen@ttu.edu,* [2]*delong.zuo@ttu.edu,* [3]*zhuo.tang@ttu.edu,* [4]*darryl.james@ttu.edu*

SUMMARY
Tornado-like loading on a low-rise building model by a single-celled vortex and a two-celled vortex was investigated based on testing in a tornado simulator. The results show that the coefficients of the mean peak forces caused by the single-celled vortex are significantly larger than the coefficients of those caused by the two-celled vortex largely due to the larger pressure drop inside the single-celled vortex. In addition, it was found out that the tornado-like loading depends on the path and speed of the translational motion between the vortex and the model. In particular, when the model translates through the center of the vortex, the mean peak forces decrease with increasing translation speed.

Keywords: tornadic loading, low-rise building, tornado-like vortex

1. GENERAL INSTRUCTIONS

Tornadoes are among the most destructive natural hazards and cause tremendous loss of properties and lives each year. Many studies have been conducted to investigate tornado-like loading on buildings (e.g., Case et al, 2014; Haan et al, 2010; Kopp and Wu, 2020; Letchford et al, 2015; Roueche et al, 2020; Wang et al, 2018). The main findings include: (1) The mean peak loading induced by tornado-like vortices can be significantly larger than that induced by the straight-line winds; (2) Leakages in the building envelope lead to pressure drop inside the building that results in a reduction in the uplift force; the effect of leakages could be negligible when a dominant opening exists; (3) The location and orientation of the building relative to a vortex, the roof geometry and the path and speed of vortex translation can significantly affect the loading. In this study, a building model was tested in a single-celled vortex and a two-celled vortex generated in a tornado simulator. The data from the testing are used to reveal the characteristics of the tornado-like loading, the differences between the loading by the two vortices, and the dependence of the loading on the model translation path and speed.

2. EXPERIMENTAL SETUP

2.1 Characteristics of tornado-like vortices

The experiment was conducted in a single-celled vortex and a two-celled vortex generated in the tornado simulator at Texas Tech University. Measurements of the flow velocity and the pressure on the floor were made with the center section of the simulator floor being stationary and

translating at two speeds. Table 1 shows the major characteristics of the two vortices while the floor beneath the vortices was stationary. Here r_c is the core radius taken as the radial distance from the center of the vortex to the location of the maximum mean tangential velocity.

Table 1 Characteristics of simulated vortices

Type of vortex	Swirl ratio (S)	Internal aspect ratio (a)	Radial Reynolds number (Re_r)	Maximum mean tangential velocity ($\overline{V}_{\theta,\,max}$, m/s)	Core radius (r_c, cm)
Single-celled	0.17	0.5	5.1×10^5	11.2	8
Two-celled	0.83	0.5	6.5×10^5	11.5	46

Detailed characteristics of the flow fields are not presented herein. Instead, some characteristics of the pressures on the floor underneath the vortices, which reflect the characteristics of the flows, are presented. The pressure coefficient defined as $C_P = (P\text{-}P_{ref})/(0.5\rho\overline{V}^2_{\theta,\,max})$, is used to represent the pressures. Here P is the pressure at the measurement location, P_{ref} is the reference pressure, taken as the barometric pressure under the simulator floor, ρ is the air density, and $\overline{V}_{\theta,\,max}$ is the maximum mean tangential velocity of the flow when the floor is stationary. Figure 1 (a) and (b) show the radial profiles of the first four statistical moments of the pressures on the floor while the floor is stationary. Here r is the radial position from the center of the vortex, $\overline{C}_P$ is the mean value and $\widetilde{C}_P$ is the standard deviation of the pressure. Figure 1 (a) suggests that in regions close to and inside the cores of the vortices, both the mean value and standard deviation of the pressure deficit caused by the single-celled vortex are significantly larger than those of the pressure deficit caused by the two-celled vortex. Figure 1 (b) shows that the pressures caused by the two vortices can be highly non-Gaussian and that the regions over which the pressure deviates the most from the Gaussian distribution are different for the two vortices.

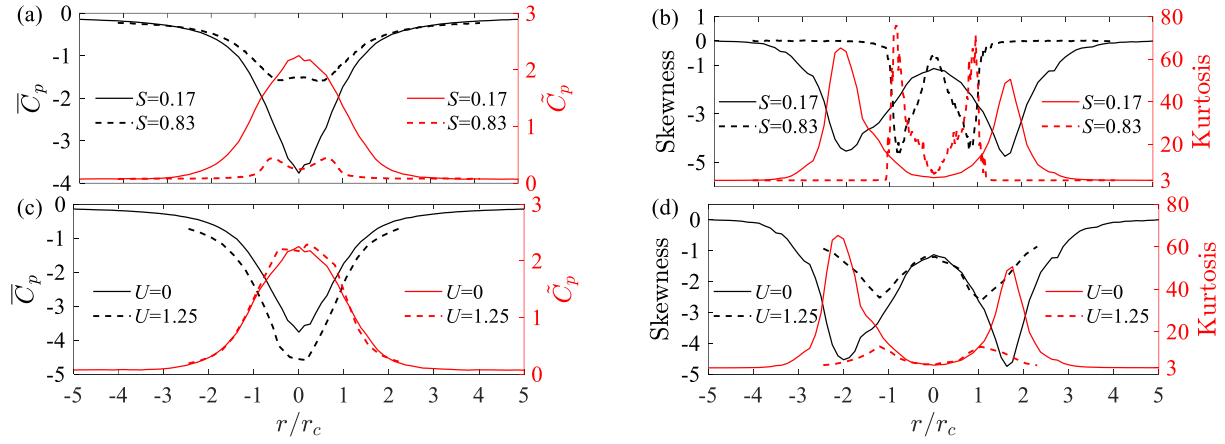

Figure 1 (a) and (b) Characteristics of the pressures on the stationary floor under the two vortices and (c) and (d) the effect of translation on the characteristics of the pressures on the floor under the single-celled vortex

The measurements suggest that the translation of the floor only has insignificant effect on the characteristics of the pressure deficit caused by the two-celled vortex. However, the pressure deficit caused by the single-celled vortex is significantly affected by floor translation. The floor translation can significantly shift the position of the point of the maximum mean static pressure deficit caused by this vortex. Figure 1 (c) and (d) show the effects of floor translation at speed U = 1.25 m/s on the pressures under the single-celled vortex. Here the profiles of the pressures on

the translating floor are at points on a line that passes through the point of the maximum mean pressure deficit, which is taken as the center of the vortex at the floor level and is perpendicular to the translation direction. It is seen that the translation substantially increases the mean pressure deficit and significantly affects the characteristics of pressure fluctuation.

2.2 Building model and test configurations

The building model is 13.8 cm, 9.3 cm, 3.9 cm, and 4.0 cm, respectively, in length, width, eve height, and roof ridge height. Figure 2 shows the configurations when the model translates along path lines $y/r_c = 0$ and $y/r_c = 1$ through the vortices rotating in the counterclockwise direction. A fixed coordinate system x- y with its origin at the center of the two vortices at the floor level and the x axis being along the translation direction is defined for locating the model. During the tests, pressures at 204 taps on the model were measured by a Scanivalve system, which were used to obtain the forces acting on the model. The tests were repeated 200 times to allow the estimation of loading statistics.

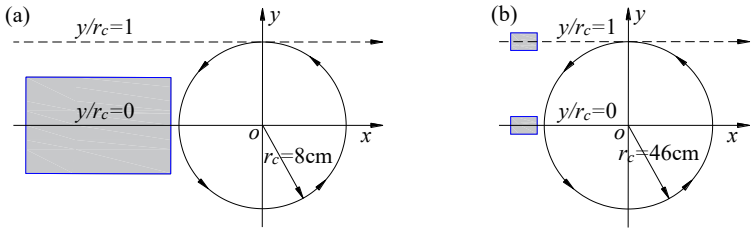

Figure 2 Schematic illustration of representative test configurations (a) $S = 0.17$ and (b) $S = 0.83$

3. RESULTS AND DISCUSSIONS

Figure 3 shows the position-varying first four moments of the uplift force coefficient (C_{Fz})when the model translates at speed $U = 1.25$ m/s along the two path lines. Figure 3 (a) and (b) suggests that for $S = 0.83$ and $y/r_c = 0$, the mean value ($\overline{C}_{Fz}$) and standard deviation ($\widetilde{C}_{Fz}$) of the uplift force reach the maximum at a location near $x/r_c = \pm 1$ because the horizontal wind velocities around these radial locations are significantly larger than those at other radial locations, and the pressures on the roof of the model here are significantly affected by flow separation from the roof edges, which creates larger mean negative pressures and fluctuations. Also, the maximum mean value and standard deviation of the uplift force coefficients for $S = 0.17$ are about as 1.5 times as those for $S = 0.83$ when the model translates along path line $y/r_c = 0$, partly because of the larger pressure deficit and fluctuation of the flow inside the single-celled vortex. Also, For $S = 0.17$, the maximum mean uplift force for $y/r_c = 0$ is larger than that for $y/r_c = 1$, which is also partly due to the larger pressure drop and fluctuation. Figure 3 (c) and (d) indicates that for $S = 0.83$, the uplift force inside the vortex can be highly non-Gaussian due to the non-Gaussian characteristics of the flow, and it deviates more from Gaussian when the model translates along path line $y/r_c = 0$. For $S = 0.17$, the range of the normalized position over which the uplift force shows non-Gaussian property is much wider compared with that for $S = 0.83$.

Figure 4 shows the mean peak force coefficients in the x and z directions ($\widehat{C}_{Fx}$ and $\widehat{C}_{Fz}$) when the model translates through the two vortices along two path lines at various speeds. For given translation path and speed, the mean peak force coefficients due to the single-celled vortex are

larger than those due to the two-celled vortex partly due to the larger static pressure deficits in the core area in the single-celled vortex. The mean peak force coefficients are smaller when the model translates along path line y/r_c = 1 than when it translates through the center of the vortex again partly because of the larger static pressure deficits inside the vortices. In addition, when the model translates along path line y/r_c = 0, the mean peak forces decrease with increasing translation speed. However, the effect of the translation speed on the mean peak forces is insignificant when the model translates along path line y/r_c = 1 through the two-celled vortex, although the mean peak forces caused by the single-celled vortex still decrease with increasing translation speed.

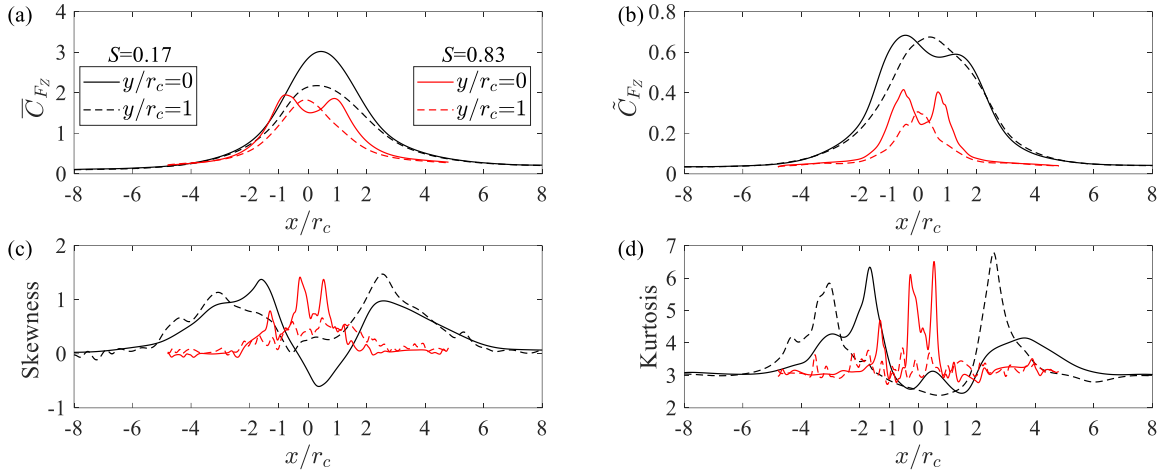

Figure 3 Position varying statistics of uplift force coefficient C_{Fz}

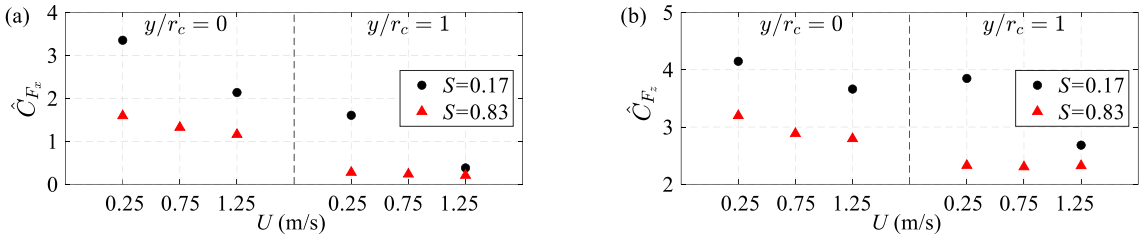

Figure 4 Mean extreme force coefficients (a) $\widehat{C}_{Fx}$ and (b) $\widehat{C}_{Fz}$

REFERENCES

Case, J., Sarkar, P., Sritharan, S., 2014. Effect of low-rise building geometry on tornado-induced loads. Journal of Wind Engineering and Industrial Aerodynamics 133, 124-134.

Haan, F.L., Balaramudu Vasanth, K., Sarkar, P.P., 2010. Tornado-induced wind loads on a low-rise building. Journal of Structural Engineering 136, 106-116.

Kopp, G.A., Wu, C.H., 2020. A framework to compare wind loads on low-rise buildings in tornadoes and atmospheric boundary layers. Journal of Wind Engineering and Industrial Aerodynamics 204, 104269.

Letchford, C., Levitz, B., James, D., 2015. Internal pressure dynamics in simulated tornadoes. Structures Congress 2015, 2689-2701.

Roueche, D.B., Prevatt, D.O., Haan, F.L., 2020. Tornado-induced and straight-line wind loads on a low-rise building with consideration of internal pressure. University Faculty Publications 163.

Wang, J., Cao, S., Pang, W., Cao, J., 2018. Experimental study on tornado-induced wind pressures on a cubic building with openings. Journal of Structural Engineering 144, 04017206.